Journal of Power Sources, 43–44 (1993) 539–546

Studies of spinel $LiCr_xMn_{2-x}O_4$ for secondary lithium battery

Wang Baochen, Xia Yongyao, Feng Li and Zhao Dongjiang
Changchun Institute of Applied Chemistry, Academia Sinica, Changchun 130022 (China)

Abstract

X-ray and electrochemical studies of spinel-related manganese chromium oxides, $LiCr_xMn_{2-x}O_4$ ($0 \leqslant x < 1$) were carried out in a lithium nonaqueous cell. X-ray diffraction spectra indicated that the substitution of manganese in $LiMn_2O_4$ by trivalent transition metals (Cr^{3+}) cause the linear decrease of lattice parameter with the x in the $LiCr_xMn_{2-x}O_4$. Some discharge-capacity loss was obtained due to the lattice contraction of $LiCr_xMn_{2-x}O_4$, but it has a better rechargeability than $LiMn_2O_4$. Cyclic voltammetry and electrochemical impedance experiments have shown that the excellent rechargeability of $LiCr_xMn_{2-x}O_4$ may be attributed to the good reversibility of the change in its crystal structure for the insertion and extraction of lithium ions.

Introduction

In recent years, manganese dioxide has been widely used as a cathode in a lithium nonaqueous cell. A detailed electrochemical and structural investigation on spinel $LiMn_2O_4$ has been reported because of its good rechargeability [1–4]. The substitution of manganese in $LiMn_2O_4$ by trivalent transition metal may also effect its structure and rechargeability. In this paper, we reported the results of the electrochemical discharge, X-ray diffraction, cyclic voltammetry and electrochemical impedance spectrum of $LiCr_xMn_{2-x}O_4$ in which Mn^{3+} at the octahedral site was substituted for Cr^{3+} ion.

Experimental

Spinel $LiCr_xMn_{2-x}O_4$ ($0 \leqslant x < 1$) was prepared by heat-treating the mixture of Li_2CO_3, Mn_2O_3 and CrO_3 at a given atomic ratio Li:Mn:Cr, at 650 °C for 12 h, then at 900 °C for 24 h.

The crystal structure was determined by X-ray diffraction analysis (XRD) (Cu Kα), the x values of $LiCr_xMn_{2-x}O_4$ were obtained by chemical analysis.

The cathode was prepared from a mixture of 88 wt.% active material (w/o), 10 wt.% acetylene black, and 2 wt.% Teflon organic binder pressing on a 1 cm^2 nickel screen. The electrolyte was 1 M $LiClO_4$/propylene carbonate (PC)–1,2-dimethoxyethane (DME) (1:1) solution.

The experimental cells were assembled in a dry box (VAC). The discharge and charge experiments were examined with a flat cell, consisting of lithium foil anode,

0378-7753/93/$6.00

studied cathode and porous polypropylene as a separator. The cyclic voltammetry and a.c. impedance experiments were conducted in a three-electrode cell, lithium foil served as a reference and counter electrodes. The impedance measurements were carried out by a 5208 two-phase lock-in analyzer and potentiostat/galvanostat Model 273 controlled by IBM-PC microcomputer. Experiments were usually performed in the frequency range of 10^5 Hz–0.1 Hz.

Results and discussion

Table 1 gives the results of the chemical analysis of the mixed metal oxides. The prepared $LiCr_xMn_{2-x}O_4$ ($0 \leqslant x < 1$) was characterized by XRD as shown in Fig. 1. The crystal structure of $LiCr_xMn_{2-x}O_4$ was determined to be a cubic lattice having a space group Fd3m(oh^7) in which Mn^{3+}, Mn^{4+} and Cr^{3+} ions are at 16(d) and O^{2-} ions are at 32(c) site identical to $LiMn_2O_4$ structure, but the lattice constants are different. The determined values of lattice constants are smaller than that of $LiMn_2O_4$ as described in Table 2. The lattice constant decreases as a linear function of molar chromium-doped in $LiCr_xMn_{2-x}O_4$ as displayed in Fig. 2.

Figure 3 shows the continuous discharge curve of $LiMn_2O_4$ and $LiCr_{0.4}Mn_{1.6}O_4$ at 250 $\mu A/cm^2$ at 25 °C. The cutoff voltage was 2.0 V. The working voltage of $LiMn_2O_4$

TABLE 1

Chemical analysis of the mixed metal oxides $LiCr_xMn_{2-x}O_4$

Target materials	Analytical values (wt.%)			Approximate chemical composition
	Li	Cr	Mn	
$LiMn_2O_4$	3.85	0	60.96	$Li_{1.00}Mn_{2.00}O_{3.97}$
$LiCr_{0.2}Mn_{1.8}O_4$	3.78	5.20	55.30	$Li_{0.98}Cr_{0.18}Mn_{1.82}O_{3.98}$
$LiCr_{0.4}Mn_{1.6}O_4$	3.88	11.34	49.52	$Li_{1.00}Cr_{0.39}Mn_{1.61}O_{3.94}$
$LiCr_{0.6}Mn_{1.4}O_4$	3.87	17.00	44.03	$Li_{0.99}Cr_{0.58}Mn_{1.42}O_{3.89}$
$LiCr_{0.8}Mn_{1.2}O_4$	3.80	22.30	38.49	$Li_{0.97}Cr_{0.76}Mn_{1.24}O_{3.92}$

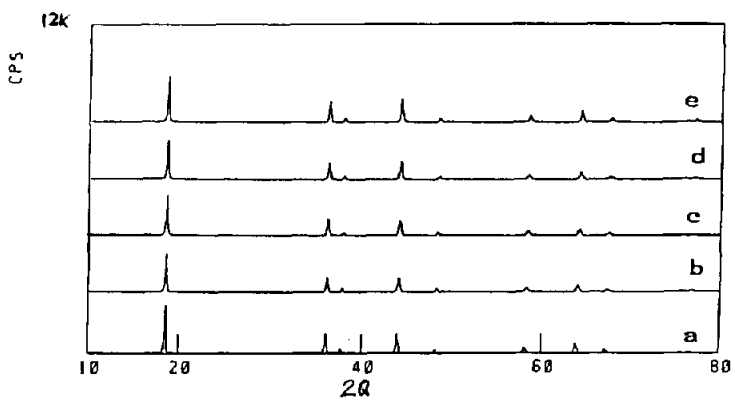

Fig. 1. X-ray diffractional pattern of $LiCr_xMn_{2-x}O_4$ ($0 \leqslant x < 1$) (a) $x=0$; (b) $x=0.2$; (c) $x=0.4$; (d) $x=0.6$, and (e) $x=0.8$.

TABLE 2

Analysis of X-ray diffractional data of Fig. 1

Sample		$LiMn_2O_4$		$LiCr_{0.2}Mn_{1.8}O_4$		$LiCr_{0.4}Mn_{1.6}O_4$		$LiCr_{0.6}Mn_{1.4}O_4$		$LiCr_{0.8}Mn_{1.2}O_4$	
Unit cell (V)	a_0 (Å) 10^2 Å^3	8.242 5.599		8.231 5.574		8.216 5.546		8.204 5.527		8.190 5.493	
Peak no.	hkl	d_{obs}	d_{cal}	d_{obs}	d_{cal}	d_{obs}	d_{cal}	d_{obs}	d_{cal}	d_{obs}	d_{cal}
1	111	4.760	4.759	4.756	4.752	4.751	4.744	4.741	4.737	4.731	4.728
2	311	2.486	2.485	2.482	2.482	2.478	2.477	2.474	2.474	2.470	2.469
3	222	2.379	2.379	2.378	2.376	2.372	2.372	2.369	2.368	2.366	2.364
4	400	2.061	2.060	2.058	2.058	2.053	2.054	2.050	2.051	2.048	2.047
5	331	1.891	1.891	1.889	1.888	1.884	1.885	1.882	1.882	1.879	1.879
6	511	1.586	1.586	1.584	1.584	1.581	1.581	1.578	1.579	1.576	1.576
7	440	1.457	1.457	1.455	1.455	1.452	1.452	1.449	1.450	1.447	1.448
8	531	1.393	1.393	1.391	1.391	1.389	1.389	1.386	1.387	1.384	1.384
9	533	1.256	1.257	1.255	1.255	1.253	1.253	1.251	1.251	1.249	1.249
10	622	1.242	1.243	1.239	1.241	1.238	1.239	1.235	1.237	1.234	1.235

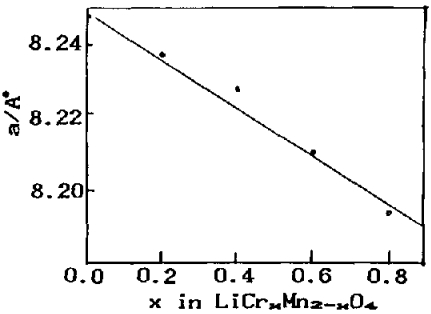

Fig. 2. Lattice constants of $LiCr_xMn_{2-x}O_4$ ($0 \leqslant x < 1$).

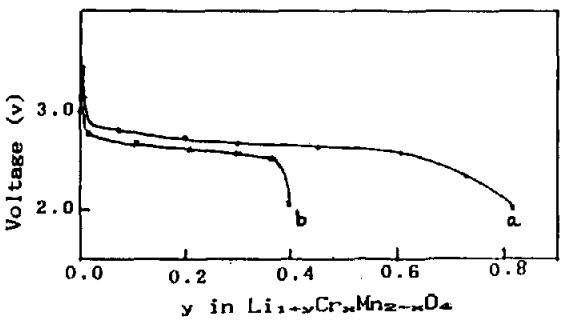

Fig. 3. Discharge curve of (a) $LiMn_2O_4$ and (b) $LiCr_{0.4}Mn_{1.6}O_4$; discharge current: 250 $\mu A/cm^2$.

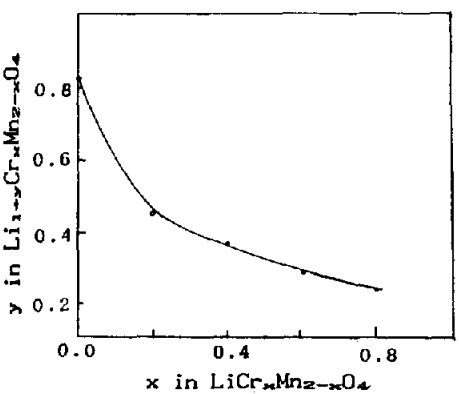

Fig. 4. Discharge capacities of $LiCr_xMn_{2-x}O_4$.

was ~100 mV higher than that of $LiCr_{0.4}Mn_{1.6}O_4$. Both samples exhibited a flat portion in the discharge curve at 2.75 and 2.65 V for $LiMn_2O_4$ and $LiCr_{0.4}Mn_{1.6}O_4$, respectively. The discharge capacities were corresponding to 120 and 50 mA h/g for $LiMn_2O_4$ and $LiCr_{0.4}Mn_{1.6}O_4$. The discharge capacities of $LiCr_xMn_{2-x}O_4$ decrease as a function of the amount of chromium doped in $LiCr_xMn_{2-x}O_4$ shown in Fig. 4. The possible explanation was that the contraction of lattice in chromium-doped samples was not favored for Li^+ insertion.

Cycle tests were carried out to characterize the rechargeability of $LiMn_2O_4$ and $LiCr_{0.4}Mn_{1.6}O_4$ in a voltage range between 2.0 and 3.8 V. Figure 5 shows the examples of rechargeable behavior of $LiMn_2O_4$ and $LiCr_{0.4}Mn_{1.6}O_4$. The shape of the charge and discharge curves obtained from $LiMn_2O_4$ and $LiCr_xMn_{2-x}O_4$ was quite similar. But the working voltage and first discharge capacity of $LiMn_2O_4$ was higher than that of $LiCr_{0.4}Mn_{1.6}O_4$. However, less rechargeable capacity loss was obtained for $LiCr_{0.4}Mn_{1.6}O_4$ than for $LiMn_2O_4$, therefore the $LiCr_{0.4}Mn_{1.6}O_4$ has a better rechargeability, which may be contributed to the good reversible change of its crystal structure for the insertion and extraction of lithium ions.

In order to confirm the rechargeability of $LiMn_2O_4$ and $LiCr_{0.4}Mn_{1.6}O_4$, cyclic voltammetry measurements were taken, and the results are presented in Fig. 6. In Fig. 6(a) the oxidation peak 1 at 3.5 V corresponds to the reaction reported in the literature [5]:

$$(Li_2)_{oct}(Mn_2)_{oct}O_4 \longrightarrow Li_{tet}(Mn_2)_{oct}O_4 \qquad (1)$$

rock salt composition spinel composition

The cyclic voltammogram of $LiCr_{0.4}Mn_{1.6}O_4$ shows similar feature to the $LiMn_2O_4$, the lithium ions insertion and extraction reaction associated with $LiCr_{0.4}Mn_{1.6}O_4$ may believed to be:

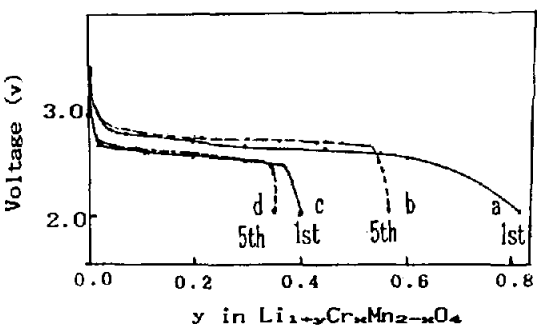

Fig. 5. Cycle performances of $LiMn_2O_4$ and $LiCr_{0.4}Mn_{1.6}O_4$: (a), (b) for $LiMn_2O_4$; (c), (d) for $LiCr_{0.4}Mn_{1.6}O_4$.

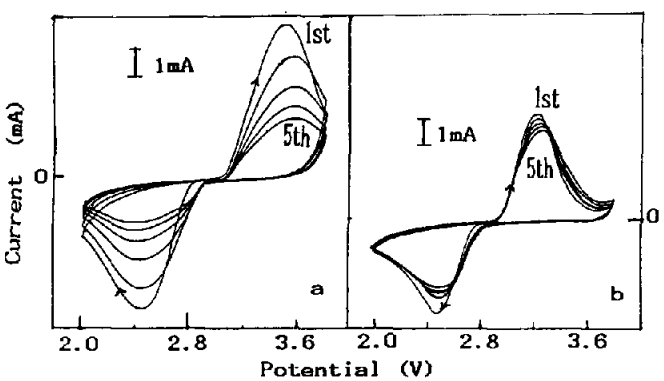

Fig. 6. Cyclic voltammogram of (a) $LiMn_2O_4$ and (b) $LiCr_{0.4}Mn_{1.6}O_4$; scan rate: 1 mV/s.

$$(Li_2)_{oct}(Cr_{0.4}Mn_{1.6})_{oct}O_4 \longrightarrow Li_{tet}(Cr_{0.4}Mn_{1.6})_{oct}O_4 \quad (2)$$

rock salt composition spinel composition

There was an apparent difference between $LiMn_2O_4$ and $LiCr_{0.4}Mn_{1.6}O_4$, the peak current of $LiMn_2O_4$ decreases faster than that of $LiCr_{0.4}Mn_{1.6}O_4$ as a the cycle numbers increase. This also indicated that the $LiCr_{0.4}Mn_{1.6}O_4$ has a good rechargeability.

The problem of the a.c. impedance spectrum for a simple insertion electrode reaction with either charge-transfer or diffusion-limited kinetics, involving desolvation and transfer of an ion from the electrolyte has been considered by several authors [6–8]. The equivalent circuit is a series combination of the charge-transfer resistance, R_{ct}, and the Warburg diffusion impedance, Z_w, shunted by the double-layer capacity, C_{dl}. The diffusion-controlled migration, in the electrolyte or the solid, may be described by the Warburg impedance [7]:

$$Z_w = Z(1-j)\omega^{-1/2} \quad (3)$$

$$|z| = \left|\frac{V_m(dE/dy)}{zFaD^{1/2}}\right| \omega^{-1/2} \quad (4)$$

The so-called chemical diffusion coefficient D can be determined from eqn. (4), V_m is the molar volume of the solid and dE/dy is the slope of the open-circuit voltage E versus mobile ion concentration obtained by differentiating the coulombmetic titration curve. Figures 7 and 8 show the complex impedance data change with a progressive reduction and oxidation of $LiMn_2O_4$ and $LiCr_{0.4}Mn_{1.6}O_4$. It may be clearly seen that the impedance diagrams show a well-defined response with a semicircle at high frequency which was related to electrolyte solution/cathode interface (which is associated with a charge resistance, R_{ct}) and a 45° Warburg line at low frequency (related to the diffusion of the intercalated lithium into the $LiCr_xMn_{2-x}O_4$). The diameter of semicircle increased as the discharge proceeds, which indicated the charge-transfer controlled kinetics became difficult as more lithium is added to the lattice. At low frequency, the rate of lithium intercalation is always diffusion controlled, as lithium ions insertion lattice increases, the diffusion coefficient is decreasing. The values of chemical diffusion coefficient D and charge-transfer resistance R_{ct} were analyzed (Table 3). It is clear that the chemical diffusion coefficient D of the state from (b) to (d) could not be determined, because the value of dE/dy is equal to zero due to the two-phase reaction [9], but D can be obtained by potentiostatic or galvanostatic pulse measurements [10,

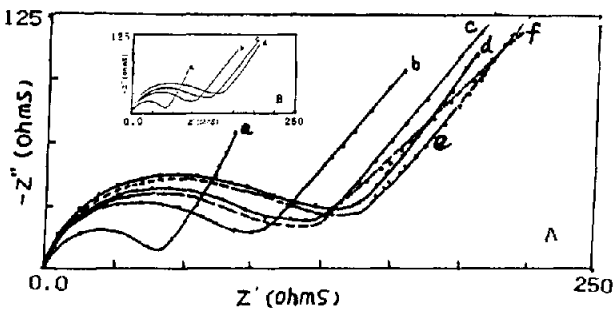

Fig. 7. (A) A.c. impedance spectrum for different discharge and charge depth of $Li_{1+x}Mn_2O_4$: (a) $x=0$; (b) $x=0.2$; (c) $x=0.5$; (d) $x=0.8$; (e) after discharge to $x=0.8$ then charge to $x=0.5$, and (f) further charge to $x=0.2$. (B) only represents the discharge states of (A).

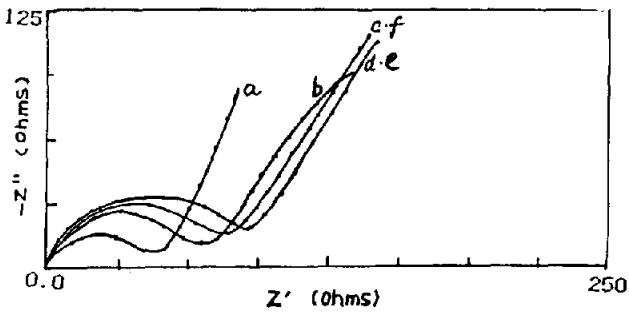

Fig. 8. A.c. impedance spectrum for different discharge and charge depth of $Li_{1+x}Cr_{0.4}Mn_{1.6}O_4$: (a) $x=0$; (b) $x=0.2$; (c) $x=0.4$; (d) $x=0.6$; (e) discharge to $x=0.6$ then charge to $x=0.4$, and (f) further charge to $x=0.2$.

TABLE 3

Thermodynamic and kinetic data of analysis of Figs. 7 and 8

Samples x y in $Li_{1+y}Cr_xMn_{2-x}O_4$		Voltage vs. Li (V)	dE/dy	R_{ct} (Ω)	D (cm^2/sec)
$x=0$	$y=1.0$	3.42	2.36	55	1.15×10^{-10}
	$y=1.2$	3.00	0.52	100	2.90×10^{-12}
	$y=1.5$	2.98	0.00	140	
	$y=1.8$	2.97	0.00	155	
	$y=1.5$[a]	3.07	0.00	150	
	$y=1.2$[a]	3.40	0.00	135	
$x=0.4$	$y=1.0$	3.30	2.27	50	3.30×10^{-10}
	$y=1.2$	2.87	0.62	75	3.67×10^{-12}
	$y=1.4$	2.86	0.00	80	
	$y=1.6$	2.83	0.00	95	
	$y=1.4$[a]	2.87	0.00	95	
	$y=1.2$[a]	3.00	0.00	80	

[a]Discharge then charge.

11], which will be reported in another paper. Comparing Figs. 7 and 8, we can see the impedance diagrams changes are smaller either in R_{ct} or D for $LiCr_{0.4}Mn_{1.6}O_4$, and the diagrams of charge state does not change so much, which also indicates that $LiCr_xMn_{2-x}O_4$ has a good reversible structure for lithium ions insertion or extraction.

Conclusions

This paper has shown that the substitution of manganese (Mn^{3+}) at 16(d) in $LiMn_2O_4$ by trivalent transition metal ion (Cr^{3+}) which has a little larger ion diameter than that of Mn^{3+}, decreased the lattice constant. This leads to a capacity loss, but the rechargeability increases. Several electrochemical studies have shown that this phenomenon may contribute to the good reversibility of the crystal structure $LiCr_xMn_{2-x}O_4$ for the insertion and extraction of lithium ions.

Acknowledgement

This work has been supported by the National Natural Science Foundation of China.

References

1 H. Iked, *4th Int. Meet. Lithium Batteries, Vancouver, BC, May 24–27, 1988,* p. 126.
2 D. G. Wickkam and W. J. Croft, *J. Phys. Chem. Solid, 7* (1958) 359.
3 M. M. Tackarary and A. de Dock, *J. Solid State Chem., 74* (1988) 414.
4 M. M. Tackarary, W. I. F. David, P. G. Bruce and J. B. Goodenough, *Mater. Res. Bull., 18* (1983) 461.
5 M. H. Rossouw, A. de Kock, L. A. de Picciotto and M. M. Thackeray, *Mater. Res. Bull., 25* (1990) 173.
6 J. Jacovsen, K. West, B. Zachau-Christiansen and S. Atlung, *Electrochim. Acta, 30* (1985) 1205.
7 C. Ho, I. D. Raistrick and R. A. Huggins, *J. Electrochem. Soc., 127* (1980) 434.
8 M. G. S. R. Thomas, P. G. Bruce and J. B. Goodenough, *J. Electrochem. Soc., 132* (1985) 1521.
9 T. Ohzuku, M. Kitagawa and T. Hirai, *J. Electrochem. Soc., 137* (1990) 771.
10 W. P. Weppner and R. A. Huggins, *J. Electrochem. Soc., 124* (1977) 1569.
11 M. Green, *Thin Solid Films, 50* (1978) 145.